Assessment of the Nonlinearity Tolerance of Different Modulation Schemes for Millimeter-Wave Fiber-Radio Systems Using MZ Modulators

Sen Lin Zhang, *Member, IEEE,* Phil M. Lane, *Member, IEEE,* and John J. O'Reilly

***Abstract*— The nonlinearity tolerance of several higher order modulation schemes, which make efficient use of transmission bandwidth, such as 8-PSK, 16-QAM, and 64-QAM, has been assessed for millimeter-wave fiber-radio systems using a Mach–Zehnder (MZ) modulator for the modulation of an optical carrier. Some other deteriorating factors, such as a bias-point shift in the MZ modulator and optical carrier leakage at the MZ filter, which is used for the separation of the two optical carriers, have also been considered. The assessment was accomplished through computer simulations. It is found that the effect of the nonlinearity of the MZ modulator is less serious for a system using 8-PSK than for a system using 16-QAM or 64-QAM, and that in the latter case, an optimal drive level exists for the modulator to achieve the best system performance. A bias-point shift, required in some deployment scenarios, degrades system performance significantly. A leakage of optical carrier to the wrong port at the MZ filter further degrades the system performance, especially for systems using the 16-QAM or 64-QAM modulation scheme.**

***Index Terms*— Fiber-radio, millimeter-wave, modulation, MZ modulation, nonlinearity.**

I. Introduction

SERVICE accessibility of broad-band communication under mobile conditions is emerging as a dominant feature for future telecommunication networks and is consequently attracting considerable attention in the literature [1]–[3]. Fiber-radio communication systems, especially those operating at millimeter-wave frequencies, will be attractive candidates for such applications [4]–[8]. Recently, the applications of millimeter-wave fiber-radio systems have been further extended to broad-band communications to fixed terminals because of the many advantages they offer such as flexibility of deployment, rapid roll-out, and cost-effectiveness. Research in this area has been financed partly by the EC ACTS projects.[1]

For millimeter-wave fiber-radio systems, it is an appropriate approach to generate the millimeter-wave signal at the antenna site by the beating on a photodiode of two optical carriers which are separated by the required frequency. For data transmission, an MZ modulator is currently used for the modulation of one of the optical carriers. However, an MZ modulator shows significant nonlinearity when a large modulating signal is applied to it to achieve efficient optical to millimeter-wave signal conversion. The system performance of a millimeter-wave fiber-radio system may be impacted by this nonlinearity and the performance degradation depends on the amplitude of the modulating signal applied to the MZ modulator, the bias point of the MZ modulator, the modulation scheme used in the system and single-channel or multichannel operation. The leakage of optical carriers at the MZ filter [9], which is used to separate the two optical carriers, may also affect the system performance. System studies should be carried out to assess and compare the effects of all the deteriorating factors and to find the best modulation scheme for such systems.

In this paper, several modulation schemes such as 8-PSK, 16-QAM, and 64-QAM, which we propose for high data-rate applications, have been evaluated, taking into account the effects of all the above-mentioned deteriorating factors. The evaluation has been carried out by system simulations using a modeling platform we developed for millimeter-wave fiber-radio systems. Both of the received-signal eye-opening and symbol-error rate have been presented. Of the three modulation schemes, 8-PSK is found to be much less affected by the nonlinearity of an MZ modulator than 16-QAM and 64-QAM, and for the latter modulation schemes, an optimal drive level for the MZ modulator exists for best system performance. A bias-point shift significantly degrades system performance. A leakage of optical carrier to the wrong ports at the MZ filter further degrades system performance, especially for 16-QAM and 64-QAM. The results and the modeling platform should provide a basis for assessing the performance of millimeter-wave fiber-radio systems under various deteriorating affects and for optimizing the performance of such systems.

II. System Configuration

The deployment block diagram of a millimeter-wave fiber-radio system, which relates to the field trial of the EC Advanced Communications Technologies & Services (ACTS) project AC083: Fiber Radio ATM Networks and Services (FRANS), is shown in Fig. 1. The data signal to be transmitted

Manuscript received December 2, 1996; revised April 28, 1997. This work was supported in part by the U.K. Engineering and Physical Science Research Council and in part by the EC ACTS program in connection with project AC083, FRANS: Fiber Radio ATM Networks and Services.

The authors are with the Department of Electronic and Electrical Engineering, University College London, London, WC1E 7JE U.K.

Publisher Item Identifier S 0018-9480(97)06021-3.

[1] *ACTS 1995—An Overview of the Programme and Projects*, EC, Brussels, Belgium, 1995.

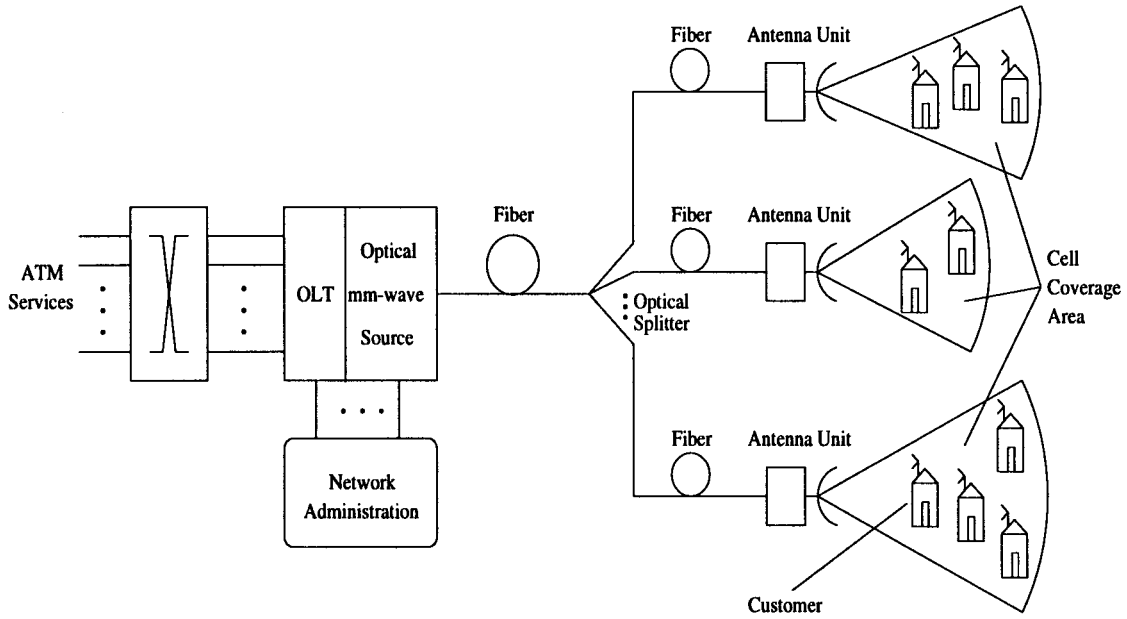

Fig. 1. System-deployment block diagram of a millimeter-wave fiber-radio system.

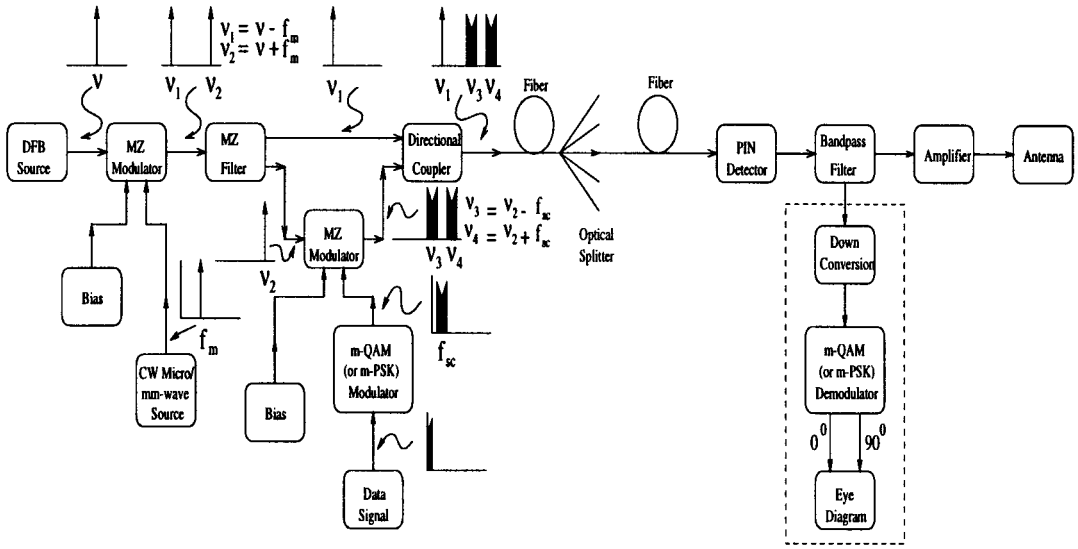

Fig. 2. System-block diagram for assessing the nonlinearity tolerance of different modulation schemes for millimeter-wave fiber-radio systems using MZ modulators.

through the fiber-radio system is acquired through the interface to the existing ATM network. Two optical carriers are generated by the optical millimeter-wave source and one of them is modulated by the data signal. A passive optical network links this optical millimeter-wave source to a number of antenna units and each of them serves a number of customers.

For millimeter-wave fiber-radio systems, the optical millimeter-wave source can be realized in different ways. A very attractive scheme is the one which uses a semiconductor laser and an MZ modulator to produce the two optical carriers, an MZ filter for the separation of them, and a second MZ modulator for modulating one of them [8]. The advantages of this arrangement are that: 1) only one laser is needed; 2) by biasing the MZ modulator at the right bias point, a sinusoidal drive signal of only half of the required millimeter-wave frequency is needed; and 3) phase noise on the two optical carriers produced in this way are completely correlated. Therefore, the millimeter-wave signal generated at the antenna site has very narrow linewidth [10]. A block diagram for such an optical millimeter-wave source together with the passive optical network and antenna unit is shown in Fig. 2. For efficient use of radio transmission bandwidth, the data signal from the ATM network is first modulated as an m-PSK or m-QAM signal [11] and then this signal is used as the drive signal for the second MZ modulator. As eye openings will be used to show system performance and, thereafter, to calculate the symbol-error rate of the system, a down conversion block, an m-PSK or m-QAM demodulator block, and an eye diagram block, which are all included in the rectangle drawn by a dashed line (see Fig. 2) are added to the system-block diagram

which represents the deployed system. The down conversion and demodulation in such a deployed system would be carried out at the user terminal. To simulate the system performance according to the above system-block diagram, system models are constructed on a modeling platform we developed for the simulation of millimeter-wave fiber-radio systems, which will be explained further in a later section.

III. MZ Modulator and Its Nonlinearity

For an ideal balanced MZ modulator, the output optical field and the input optical field are related by the following equation:

$$E_{\text{out}}(t) = E_{\text{in}}(t) \cdot \cos\left[\frac{\pi}{2} \cdot \frac{V_b + V_m(t)}{V_\pi}\right] \tag{1}$$

where V_b is the bias voltage applied, $V_m(t)$ is the modulating voltage applied, and V_π is the voltage necessary to induce π phase shift in one arm of the MZ modulator. To achieve the highest linear modulating efficiency, the bias point should be at $V_b/V_\pi = 2k+1$, where $k = 0, \pm1, \pm2, \cdots$. For such a case, using the expansion of a sinusoidal function by the Taylor series, (1) can be rewritten as follows:

$$E_{\text{out}}(t) = \pm E_{\text{in}}(t) \cdot \sum_{i=0}^{\infty} \frac{(-1)^i}{(2i+1)!}\left(\frac{\pi}{2} \cdot \frac{V_m(t)}{V_\pi}\right)^{2i+1} \tag{2}$$

where the sign before $E_{\text{in}}(t)$ takes positive value for $k = \pm1, \pm3, \pm5, \cdots$ and negative value for $k = 0, \pm2, \pm4, \cdots$. For small modulating-signal amplitude, that is $V_m(t)/V_\pi \ll 1$, $E_{\text{out}}(t) \approx \pm E_{\text{in}}(t) \cdot \pi/2 \cdot V_m(t)/V_\pi$, the output optical field approximately changes linearly with the modulating-signal amplitude, but for large modulating-signal amplitude, the linear approximation of the output optical field becomes invalid and higher order terms in (2) also need to be considered.

When an MZ modulator is used in combination with a semiconductor laser to produce the two optical carriers, as suggested by us, it is more convenient to assume that $(V_b + V_m(t)/V_\pi)$ in (1) takes the form of $(1+\epsilon)+\alpha\cdot\cos(\omega t)$, where ϵ and α are, respectively, normalized bias and drive levels. Then the output optical field from the MZ modulator will be

$$E_{\text{out}}(t) = E_{\text{in}} \cdot \cos(2\pi\nu_0 t) \cdot \cos\left\{\frac{\pi}{2}[(1+\epsilon) + \alpha \cdot \cos(\omega t)]\right\} \tag{3}$$

where ν_0 is the optical carrier frequency and E_{in} is the amplitude of the input optical field. Bessel-function expansion of the last term leads to

$$\begin{aligned} E_{\text{out}}(t) &= E_{\text{in}} \cdot \left\{+J_0\left(\alpha\frac{\pi}{2}\right) \cdot \cos\left[\frac{\pi}{2}(1+\epsilon)\right] \cdot \cos(2\pi\nu_0 t)\right. \\ &- J_1\left(\alpha\frac{\pi}{2}\right) \cdot \sin\left[\frac{\pi}{2}(1+\epsilon)\right] \cdot \cos(2\pi\nu_0 t \pm \omega t) \\ &+ J_2\left(\alpha\frac{\pi}{2}\right) \cdot \cos\left[\frac{\pi}{2}(1+\epsilon)\right] \cdot \cos(2\pi\nu_0 t \pm 2\omega t) \\ &\left.- J_3\left(\alpha\frac{\pi}{2}\right) \cdot \sin\left[\frac{\pi}{2}(1+\epsilon)\right] \cdot \cos(2\pi\nu_0 t \pm 3\omega t) + \cdots\right\}. \end{aligned} \tag{4}$$

Equation (4) shows the optical spectral components at the output of the MZ modulator for arbitrary bias and drive levels. For the special case when the MZ modulator is biased at $\epsilon = 0$, the central component at ν_0 is suppressed as are all the other even terms, the optical field spectrum will be dominated by two components at $2\pi\nu_0 - \omega$ and $2\pi\nu_0 + \omega$ when the modulating-signal amplitude is small and, therefore, the optical field can be approximately expressed as follows:

$$E_{\text{out}}(t) \approx -E_{\text{in}} \cdot J_1\left(\alpha\frac{\pi}{2}\right)\{\cos(2\pi\nu_0 t - \omega t) + \cos(2\pi\nu_0 t + \omega t)\}. \tag{5}$$

The mixing of these two components on a p-i-n photodiode will lead to an electrical signal at 2ω, doubling the frequency of the modulating signal applied to the MZ modulator.

IV. Higher Order Modulation Schemes of m-QAM and m-PSK

To make efficient use of the transmission bandwidth of the fiber-radio link, higher order modulation schemes such as m-QAM or m-PSK have been proposed by us for high data-rate applications.[1] For a fiber-radio system using an m-QAM or m-PSK modulation scheme, quadrature sub-carriers are first modulated by the data signal from the ATM network and then the modulated quadrature sub-carriers are used as the drive signal for the second MZ modulator to modulated the optical carrier. For an m-QAM modulator, the binary data signal is split first, and then converted to multilevel and low-pass filtered. After that, the filtered signal is used to modulate the quadrature sub-carriers, and finally the quadrature sub-carriers are combined. To demodulate the m-QAM signal at the receiver, the input signal is first split and then multiplied by the recovered sub-carriers, low-pass filtered, and regenerated. Finally, it is changed back to the binary form. An m-PSK modulator/demodulator is similar to an m-QAM modulator/demodulator except that the in-phase signal and quadrature signal are generated in such a way that the amplitude of the combined signal is constant [11].

V. Modeling Platform

To facilitate the simulation of millimeter-wave fiber-radio systems, a modeling platform supporting the key components for such systems has been developed [12] using the signal processing worksystem (SPW)[2] software package. The models for the key components are either symbols and sub-systems directly created in the block-diagram editor window by using the function blocks provided in the SPW library or custom coded blocks (CCB's) created following the procedure shown in the SPW user's guide.[2] A CCB, which is coded in C, has the advantage of calculating the output of the block in one simulation step, making the simulation of the whole system much easier. Models created include optical sources, an MZ modulator, optical filters, optical fiber, an erbium-doped fiber amplifier, a p-i-n receiver, a millimeter-wave receiver, etc. Auxiliary blocks such as different kinds of electrical filters, fast Fourier transform (FFT), inverse FFT (IFFT), vector-to-series and series-to-vector converters, etc. are provided in the SPW library. Using the modeling platform, different system configurations are easily constructed by combining key-component

[2] *Signal Processing Worksystem User's Guide*, Alta Group of Cadence Design System, Inc., Sunnyvale, CA, 1994.

TABLE I
PARAMETERS USED IN THE SYSTEM SIMULATIONS

Frequency band of millimeter-wave = 30GHz
Laser emission wavelength = 1.55μm
Modulating signal frequency (the 1st MZM) = 15GHz
Normalized modulating signal amplitude (the 1st MZM) = $\frac{0.1}{\pi/2}$
Sub-carrier frequency of higher order modulation schemes for single channel operation = 1.5GHz
Signal bit rate = 800Mbit/s
Baud rate for 8-PSK = 266.7Mbaud/s
Baud rate for 16-QAM = 200.0Mbaud/s
Baud rate for 64-QAM = 133.3Mbaud/s
Fiber core diameter = 8.0μm
Fiber loss = 0.2dB/km
Fiber length = 20km
Fiber dispersion $\beta_2 = 2.17 \times 10^{-23}$s·s/km
Sub-carrier frequencies of higher order modulation schemes for multichannel operations $f_{sc1,sc2,sc3}$ = 2.0, 2.1, 2.2 GHz (3 channels) $f_{sc1,sc2,sc3,sc4,sc5}$ = 2.0, 2.1, 2.2, 2.3, 2.4 GHz (5 channels)
Signal baud rate for multichannel operation = 30Mbaud/s

models and auxiliary blocks. As the component models can be either in time domain or in frequency domain, when the adjacent component blocks are in different domains, an FFT or IFFT block is used to perform the transfer from one domain to the other. Simulation can be directly carried out from such constructed system models. System parameters can be changed just before or during the simulation, with simulation results being available in a variety of formats for post-processing.

VI. RESULTS AND DISCUSSION

Simulations for the system configuration shown in Fig. 2 have been carried out with results shown and discussed in this section. Received-signal eye-opening and symbol-error rate are used to assess and compare system performances. Parameters used for the simulations are listed in Table I. Since we are dealing with a coherent system, the MZ modulator should be viewed as modulating the E-field [8]. Unless mentioned again, the MZ modulator is biased at the point of maximum E-field linearity V_π. We also assume the noise figure of the electrical system following the p-i-n to be 6 dB.

A. Non-Linearity Tolerance of Different Modulation Schemes

The nonlinearity tolerance of different modulation schemes will now be discussed. Fig. 3 shows the variation of received-signal eye opening with normalized modulating-signal amplitude, for which an amplitude of 1 corresponds to a phase shift of π between the two arms of the second MZ modulator. The optical output power from the laser is assumed to be 1 mW. We see that for 8-PSK modulation, the eye opening monotonically increases with the normalized modulating-signal amplitude, but for 16-QAM and 64-QAM modulation the eye opening increases first, as the signal power increases with the increased drive, and then decreases due to the effect of the nonlinearity of the MZ modulator. There exists an optimal drive level for the MZ modulator for these two modulation schemes. Compared with the 16-QAM and 64-QAM modulation, 8-PSK modulation is more tolerant to the nonlinearity. Comparing the 16-QAM and 64-QAM modulation, we see that the eye

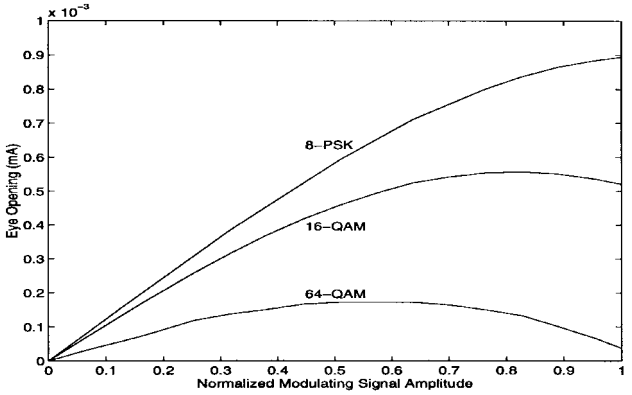

Fig. 3. Received-signal eye opening for different modulation schemes against normalized modulating-signal amplitude (optical output power from the laser equals 1 mW).

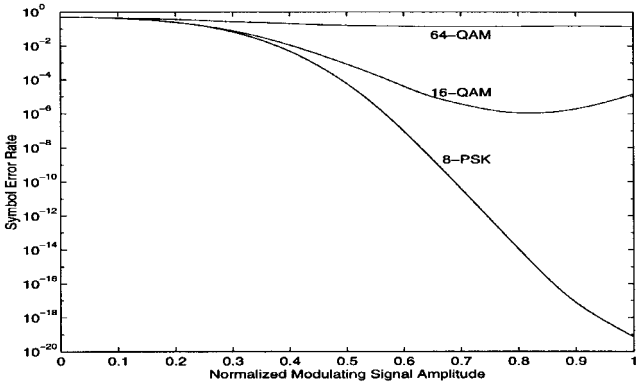

Fig. 4. Symbol-error rate for different modulation schemes for low optical carrier power of 6 μW.

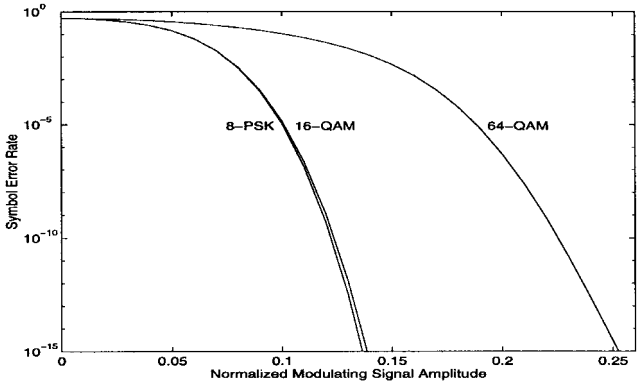

Fig. 5. Symbol-error rate for different modulation schemes for high optical carrier power of 30 μW, plotted only for small signal amplitudes.

opening for 64-QAM reaches its maximum value at a much lower modulating-signal amplitude than 16-QAM and, therefore, as expected, greater impact of the nonlinearity of an MZ modulator occurs for the 64-QAM modulation scheme.

By adopting a Gaussian approximation, the symbol-error rate for the system can be calculated using the received-signal eye opening curves shown in Fig. 3. The calculated symbol-error rates for different optical carrier powers are shown in Figs. 4 and 5. The optical powers of the unmodulated carrier at the photodiode are assumed to be 6 and 30 μW,

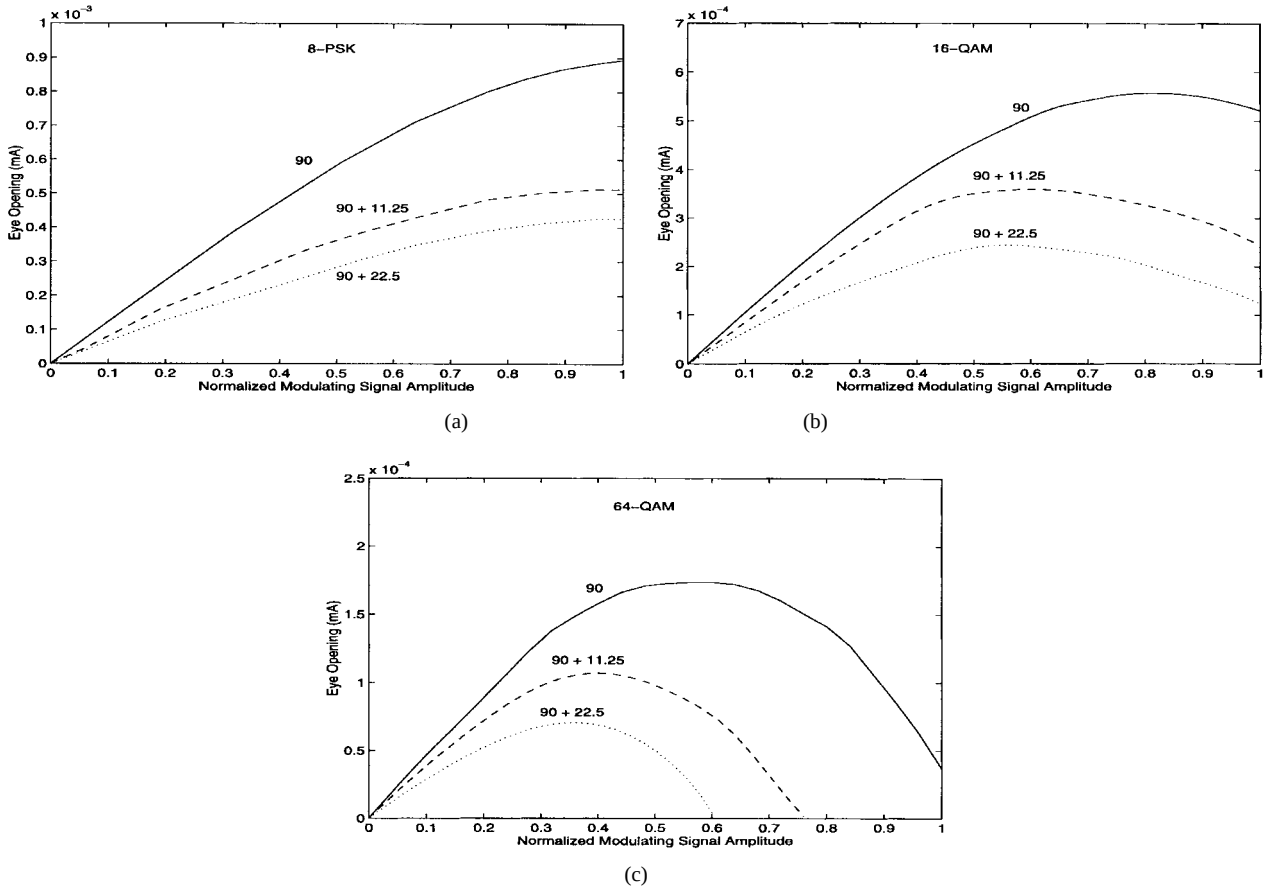

Fig. 6. Received-signal eye openings for (a) 8-PSK, (b) 16-QAM, and (c) 64-QAM modulation, with and without bias-point shift against normalized modulating-signal amplitude.

respectively, for Figs. 4 and 5. We see from Fig. 4 that when the optical carrier power is low (only for 8-PSK modulation) the symbol-error rate of the system reduces monotonically with the increase of the modulating-signal amplitude. For 16-QAM and 64-QAM modulation, the symbol-error rate decreases first with the increase of the modulating-signal amplitude and then starts to increase; therefore, for lower available optical carrier power, 8-PSK is the best of the three modulation schemes for achieving low symbol-error rate by driving the second MZ modulator with a high modulating-signal amplitude. However, when the optical carrier power is high, as shown in Fig. 5, the symbol-error rate can be reduced to a very low level for all three modulation schemes by increasing the modulating-signal amplitude. Comparing the required modulating-signal amplitude, we see that for 64-QAM modulation a much higher modulating-signal amplitude is needed to achieve the same symbol-error rate than for 8-PSK and 16-QAM modulation. For example, to achieve a symbol-error rate of 10^{-15} with 30 μW of optical carrier power, the normalized modulating-signal amplitudes are 0.136, 0.138, and 0.252, respectively, for 8-PSK, 16-QAM, and 64-QAM modulation.

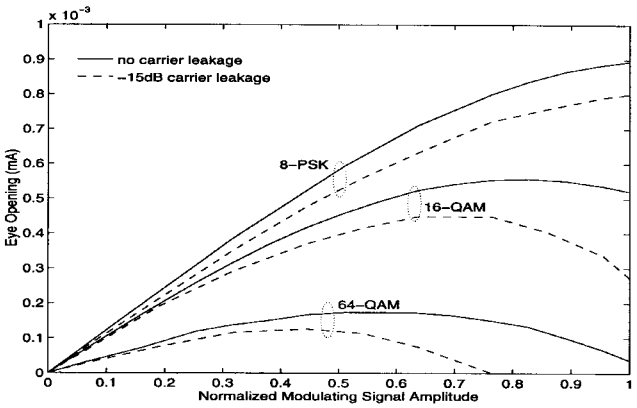

Fig. 7. Received-signal eye opening for different modulation schemes versus normalized modulating-signal amplitude considering the carrier leakage of the MZ filter.

B. Effects of a Shift of the Bias Point of an MZ Modulator

Since the effects of the nonlinearity of an MZ modulator depend on the bias point of the MZ modulator and some applications require a residual unmodulated millimeter-wave carrier at the antenna whose level is adjusted by varying the bias of the MZ modulator [8], assessment of system performance for the case when the bias point of the MZ modulator is not at V_π is also needed. Simulations of system performance for various bias points for 8-PSK, 16-QAM, and 64-QAM modulation have been carried out and the results are shown in Fig. 6. We note that with a shift in bias point the eye opening considerably reduces for all three modulation schemes and the degradation does not linearly increase with the shift in the bias point—the first $\pi/16$ shift of the biasing

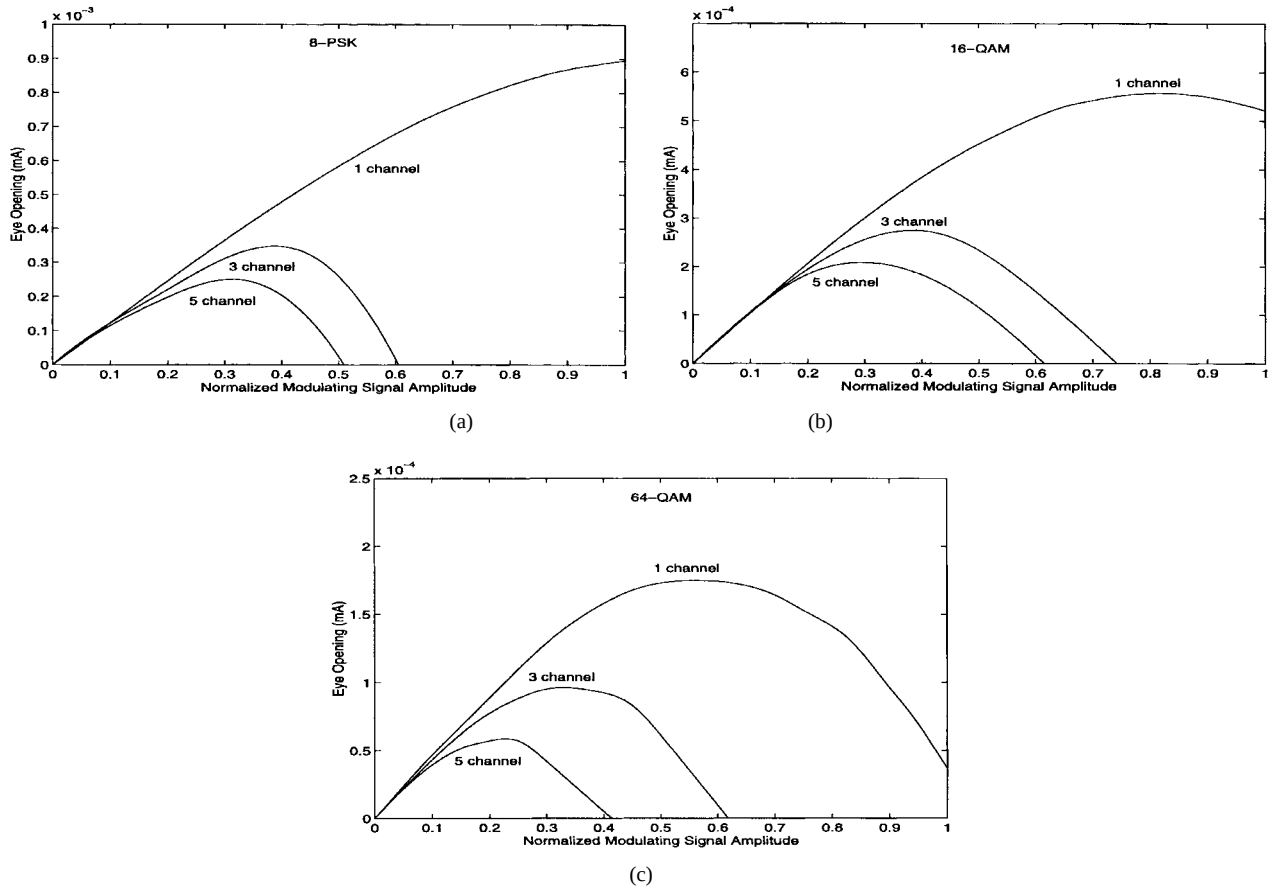

Fig. 8. Received-signal eye opening for different modulation schemes versus normalized modulating-signal amplitude for multichannel operation (a) 8-PSK, (b) 16-QAM, and (c) 64-QAM.

point degrades the system performance more than the second $\pi/16$ shift. It is also worth noting that the optimal normalized modulating-signal amplitude reduces to a lower value for 16-QAM and 64-QAM modulation. For example, for 16-QAM modulation, the optimal amplitude reduces from about 0.82 to 0.6 and 0.53, respectively, for a $\pi/16$ and a $\pi/8$ bias-point shift. For 64-QAM modulation, the optimal amplitude reduces from about 0.6 to 0.40 and 0.36, respectively, for the same bias-point shifts.

C. Effects of Carrier Leakage at the MZ Filter

Since leakage exists at the nonideal MZ filter used for separating the two optical carriers before the second MZ modulator (as shown in Fig. 2), part of the optical carriers will appear at the wrong output port. This optical carrier leakage will affect the received-signal eye opening and change the optimal normalized modulating-signal amplitude as well. System simulations have been carried out considering this leakage. For those simulations, the power level of the leaked signal is assumed to be 15 dB below the optical carrier power level. The results are illustrated in Fig. 7. We see that the effect on 8-PSK is relatively small. But the effects on 16-QAM and 64-QAM are much greater, especially at the high modulating-signal amplitude region. The optimal normalized modulating-signal amplitude also reduces from 0.81 to 0.71 for 16-QAM and from 0.57 to 0.44 for 64-QAM.

D. Multichannel Operation

Multichannel operation has also been considered for such systems. The subcarrier frequencies and signal baud rate used in the simulations are shown in Table I. The simulation results for the received-signal eye opening are shown in Fig. 8(a)–(c), respectively, for 8-PSK, 16-QAM, and 64-QAM. We see that for multichannel operation, the effect of nonlinearity of an MZ modulator is much more severe than for signal-channel operation, and only very low modulating-signal amplitude can be used to drive the MZ modulator; an optimal normalized modulating-signal amplitude now exists for 8-PSK as well, and the values for three- and five-channel operation are 0.385 and 0.31, respectively; for 16-QAM and 64-QAM, the optimal drive level of the MZ modulator significantly reduces, i.e., for 16-QAM the optimal normalized modulating-signal amplitude reduces from 0.81 to 0.38 and 0.30, respectively, for three- and five-channel operation, and for 64-QAM the optimal normalized modulating-signal amplitude reduces from 0.57 to 0.35 and 0.23, respectively, for three- and five-channel operation.

E. Bandwidth Requirement

Another important aspect which needs to be considered is the bandwidth requirement of the alternative modulation schemes. For a bit rate of 800 Mbytes/s the baud rates for 8-PSK, 16-QAM, and 64-QAM modulation are 266.7 MBd/s,

200 MBd/s, and 133.3 MBd/s, respectively. Therefore, 64-QAM modulation requires the least bandwidth, followed by 16-QAM modulation and 8-PSK modulation. From all the results shown above, we see that the performance of such systems depends on many factors such as the available optical carrier power, the available modulating-signal amplitude, the bias-point shift, single or multichannel operation, leakage of optical carrier at the MZ filter, and the bandwidth constraint. All these factors should be considered together.

VII. Summary and Conclusions

Assessment of the nonlinearity tolerance of different modulation schemes for millimeter-wave fiber-radio systems has been carried out. Through system simulations using a modeling platform developed by us, we find that of the three modulation schemes 8-PSK, 16-QAM, and 64-QAM, with low available optical power at the photodiode, 8-PSK modulation is more robust to the nonlinearity of an MZ modulator compared to 16-QAM and 64-QAM modulation. For 16-QAM and 64-QAM, there exists an optimal drive level for the MZ modulator for the best overall system performance. For a higher optical power, though, the symbol-error rate can be reduced to a very low level by increasing the modulating-signal amplitude for all three modulation schemes, much higher modulating-signal amplitude is required for 64-QAM to reach the same symbol-error rate than that for 8-PSK and 16-QAM. The effect on the system performance of a fixed shift of the bias point of the MZ modulator has also been considered. It is shown that the eye opening can be significantly reduced for all three modulation schemes; the degradation does not increase linearly with the shift in the bias point. A leakage of optical carrier to the wrong port at the MZ filter further degrades system performance, especially for 16-QAM and 64-QAM. We have also studied the cases of multichannel operation. It is shown that the effect of nonlinearity of the MZ modulator is much severer for multichannel operation than for single-channel operation and an optimal normalized modulating-signal amplitude starts to exist for 8-PSK as well. Finally, if we consider the efficient use of transmission bandwidth, 64-QAM modulation requires the least bandwidth, followed by 16-QAM modulation and 8-PSK modulation. All the above-mentioned factors must be considered together to determine the nonlinearity tolerance and the best modulation schemes for millimeter-wave fiber-radio system. The results presented, and the modeling platform we developed, should provide a basis for system designers to assess the system performance of millimeter-wave fiber-radio systems with different modulation schemes and allow the optimization of the performance of such systems.

References

[1] J. G. Gardiner, "Microwave and mm-wave engineering challenges in Pan-European communications research," in *IEEE MTT-S Int. Microwave Symp. Dig.*, San Francisco, CA, June 1966, pp. 483–486.

[2] J. L. Langston, "Multipoint™ a millimeter wave system for quick access to the information super-highway," *in IEEE MTT-S Int. Microwave Symp. Dig.*, San Francisco, CA, June 1996, pp. 1897–1900.

[3] W. Maggi and P. Polese, "Integrated broad-band communications development and implementation strategies," *IEE J. Electron. Commun. Eng.*, vol. 5, no. 5, pp. 315–320, Oct. 1993.

[4] A. Czylwik, "Optical transmission systems for the connection between central office and base stations in cellular radio systems," in *European Conf. Networks Opt. Commun. Dig. II*, Heidelberg, Germany, June 1996, pp. 279–286.

[5] J. J. O'Reilly, P. M. Lane, M. H. Capstick, H. M. Salgado, R. Heidemann, R. Hofstetter, and H. Schmuck, "RACE R2005: Microwave optical duplex antenna link," *Proc. Inst. Elect. Eng.*, vol. 140, pt. J, no. 6, pp. 385–391, Dec. 1993.

[6] R. Hofstetter, H. Schmuck, and R. Heidemann, "Dispersion effects in optical millimeter-wave systems using self-heterodyne method for transport and generation," *IEEE Trans. Microwave Theory Tech.*, vol. 43, pp. 2263–2269, Sept. 1995.

[7] D. Wake, C. R. Lima, and P. A. Davies, "Optical generation of millimeter-wave signals for fiber-radio systems using a dual-mode DFB semiconductor laser," *IEEE Trans. Microwave Theory Tech.*, vol. 43, pp. 2270–2296, Sept. 1995.

[8] J. J. O'Reilly and P. M. Lane, "Remote delivery of video services using mm-wave and optics," *J. Lightwave Technol.*, vol. 12, pp. 369–375, Feb. 1994.

[9] B. Verbeek, C. Henry, N. Olsson, K. Orlowsky, R. Kazarinov, and B. Johnson, "Integrated four-channel Mach–Zehnder multi/demultiplexer fabricated with phosphorous doped SiO_2 waveguides on Si," *J. Lightwave Technol.*, vol. 6, pp. 1011–1015, June 1988.

[10] J. J. O'Reilly, P. M. Lane, R. Heidemann, and R. Hofstetter, "Optical generation of very narrow linewidth millimeter wave signals," *Electron. Lett.*, vol. 28, no. 25, pp. 2309–2311, Dec. 1992.

[11] D. R. Smith, *Digital Transmission Systems*, 2nd ed. New York: Van Nostrand, 1993.

[12] S. L. Zhang and J. J. O'Reilly, "Simulation of fiber supported millimeter-wave communication system," in *European Simulation Congr. EUROSIM'95 Dig.*, Vienna, Austria, pp. 565–570, Sept. 1995.

Sen Lin Zhang (M'96) was born in Beijing, China, in November 1961. He received the B.Sc. and M.Sc. degrees in telecommunications from Northern Jiaotong University, Beijing, China, in 1982, and 1985, respectively, and the Ph.D. degree from the University of Wales–Bangor, U.K. in 1992.

From 1985 to 1988, he was employed by the Institute of Signalling and Communications, China Academy of Railway Sciences, undertaking research on digital communications. From 1992 to June 1994, he worked as a Research Officer with the School of Electronic Engineering and Computer Systems, University of Wales–Bangor, U.K. Since July 1994, he has been employed as a Research Fellow in the Department of Electronic and Electrical Engineering, University College London, London, U.K. He has published over 40 technical papers. His main research interests include millimeter-wave fiber-radio systems, third-generation mobile-communication systems, computer simulation of communication systems, fiber nonlinearities, and optical amplifiers and their applications in fiber communication systems.

Dr. Zhang is an associate member of the Institute of Electrical Engineers (IEE) (U.K.).

Phil M. Lane, (S'90–M'92), for a biography, see this issue, p. 1402.

John J. O'Reilly, for a photograph and biography, see this issue, p. 1402.